Regional cerebral activation accompanies sympathoexcitation in women with polycystic ovary syndrome

Andrew J Lansdown, Esther AH Warnert, Yrsa Sverrisdóttir, Richard G Wise, D. Aled Rees

Department of Endocrinology, University Hospital of Wales, Cardiff, United Kingdom (AJL); Department of Radiology, Erasmus Medical Center, Rotterdam, Netherlands (EAHW); Nuffield Department of Surgical Sciences, Medical Sciences Division, University of Oxford, Oxford, United Kingdom (YS); Cardiff University Brain Research Imaging Centre, School of Psychology, Cardiff University, Cardiff, United Kingdom (RGW); Neuroscience and Mental Health Research Institute, Cardiff University, Cardiff, CF24 4HQ United Kingdom (DAR)

Abbreviated title: Sympathetic neural activation in PCOS

Keywords: Polycystic ovary syndrome; insulin resistance; sympathetic nervous system; orbitofrontal cortex; fMRI

Correspondence: Aled Rees, Neuroscience and Mental Health Research Institute, School of Medicine, Cardiff University, Cardiff CF24 4HQ, UK. Tel +44 29 2074 5002; Fax +44 29 2074 4671; Email reesda@cf.ac.uk.

Grants: This work was supported by a Society for Endocrinology Early Career Grant to AJL.

Disclosure statement: The authors have nothing to disclose.

Abstract

Context: Polycystic ovary syndrome (PCOS) is associated with increased sympathetic nervous system (SNS) activation but the cerebral pathways involved are unclear.

Objective: To compare cerebral (blood oxygen level-dependent [BOLD] fMRI), pressor (blood pressure [BP], heart rate [HR]) and muscle sympathetic nerve activity (MSNA) responses to isometric forearm contraction (IFC) in women with PCOS and matched controls.

Design: Case-control study

Setting: Referral center

Participants: 20 subjects with PCOS (age 29.8 ± 4.8yrs, BMI 26.1 ± 4.9kg/ m²) and 20 age/BMI-matched controls (age 29.7 ± 5.0yrs, BMI 26.1 ± 4.8kg/ m²)

Main outcome measures: BP, HR, catecholamine and MSNA responses to 30% IFC. BOLD signal change modelled for blood pressure response to 30% IFC.

Results: Whilst HR and BP increased to a similar extent in both groups following IFC, MSNA burst frequency increased by 68% in the PCOS group (n=7) compared to 11.9% in controls (n=7) ($p=0.002$). Brain activation indexed by the BOLD signal in response to IFC was significantly greater in the PCOS group (n=15) compared to controls (n=15) in the right orbitofrontal cortex ($p<0.0001$). Adjustment for insulin sensitivity, but not hyperandrogenism, abolished these between-group differences.

Conclusions: Our study confirms enhanced sympathoexcitation in women with PCOS and demonstrates increased regional brain activation in response to IFC. The right orbitofrontal cortex BOLD signal change in women with PCOS is associated with insulin sensitivity. Further studies are warranted to clarify whether this may offer a novel target for cardiovascular risk reduction.

Précis

In women with PCOS, enhanced sympathoexcitation is accompanied by cerebral activation in the right orbitofrontal cortex that is influenced by insulin sensitivity.

Introduction

Polycystic ovary syndrome (PCOS) is a common metabolic disorder characterized by defects in insulin secretion and action. This leads to an increased risk of metabolic syndrome and disorders of glucose tolerance, including type 2 diabetes [1]. Women with PCOS also display a higher prevalence of cardiovascular risk markers, including dyslipidemia [2], hypertension [3] and endothelial dysfunction [4], although studies are yet to confirm if this leads to increased cardiovascular morbidity and mortality.

Sympathetic nervous system (SNS) activation may also contribute to this enhanced cardiometabolic risk [5], since conditions associated with chronic sympathoexcitation, such as obesity, hyperinsulinemia and obstructive sleep apnoea (OSA), are common in women with PCOS. In support of this, heart rate variability is altered [6-8] and heart rate and blood pressure recovery after exercise is delayed [9-10] in women with PCOS compared to matched controls, consistent with enhanced sympathetic stimulation and increased peripheral arterial resistance. Direct measurement of muscle sympathetic nerve activity (MSNA) by microneurography has also confirmed enhanced sympathetic outflow in women with PCOS compared with age- and BMI-matched controls [11-12].

The mechanisms by which this enhanced sympathetic activation occurs are not entirely clear, although both hyperinsulinemia [12] and hyperandrogenism [11] have been implicated. The origins of this activation are also uncertain, although the hypothalamus [13], brainstem [14] and higher brain centers [15] appear to be involved in regulating sympathetic tone in rodents. Contemporary imaging techniques, such as positron emission tomography [16-17] and blood oxygen level-dependent functional magnetic resonance imaging (BOLD fMRI) [18-20], facilitate neuroanatomical localization of these responses in humans, and have identified a

number of cortical and brainstem regions involved in this process. To our knowledge, similar studies have not been undertaken in metabolic disorders characterized by insulin resistance, including PCOS, in which compensatory hyperinsulinemia might be anticipated to amplify the cerebral responses to sympathoexcitation.

We hypothesized that women with PCOS would have evidence of sympathoexcitation accompanied by functional differences in higher brain centres. We therefore set out to compare cerebral (BOLD fMRI), pressor (blood pressure and heart rate) and MSNA responses to an isometric forearm contraction model of sympathoexcitation in women with PCOS and matched controls.

Materials and Methods

Participants

Patients with PCOS (n=20) were recruited from the endocrine clinic at the University Hospital of Wales, the endocrine clinic at Morriston Hospital, Swansea, and Morlais Medical Practice, Merthyr Tydfil. Diagnosis was made according to the Rotterdam criteria [21]. Congenital adrenal hyperplasia, Cushing's syndrome, androgen-secreting neoplasms, hyperprolactinemia and thyroid disease were excluded by biochemical testing. Patients were aged between 18 and 45 years. Exclusion criteria were: pregnancy and breastfeeding, hyperlipidemia or use of lipid-lowering agents, hypertension or use of anti-hypertensives, use of glucocorticoids or anti-obesity drugs, diabetes or use of antidiabetic drugs within 3 months. Patients with any contraindication to MRI were also excluded. Of the 20 women, 12 had polycystic ovaries (PCO), hyperandrogenism and anovulation, 5 had hyperandrogenism and anovulation, 2 had PCO and hyperandrogenism, and 1 had PCO and anovulation.

Healthy volunteers (n=20) were recruited as controls. For each individual patient, a control was identified matched for age (within 2 yrs) and BMI (within 2 kg/m²). Controls needed to have regular menstrual cycles (menses every 27–32 days). Their healthy state was determined by history, examination and hormonal evaluation (testosterone, androstenedione, thyroid function, prolactin). Control subjects with signs of hirsutism or with a personal history of diabetes or hypertension, or a family history of PCOS, or current pregnancy were excluded. Those with any contraindication to MRI were also excluded. Healthy volunteers were recruited by advertisement among staff and students at the University Hospital of Wales, Cardiff University and in the local press. The study was approved by Cardiff University (study sponsors), Cardiff

and Vale University Health Board and the South East Wales Research Ethics Committee (reference 12/WA/0239). All subjects gave written, informed consent.

Anthropometric and biochemical measurements

Height, weight, waist and hip circumference were measured according to our previously published protocol [22]. Blood samples were collected after an overnight fast. Serum total cholesterol and triglycerides were assayed using an Aeroset analyzer (Abbott Diagnostics). Insulin was measured using an immunometric assay specific for human insulin (Invitron), and glucose was measured using the Aeroset chemistry system (Abbott Diagnostics). Total testosterone was measured by liquid chromatography-tandem mass spectrometry (QuattroTM Premier XE triple quadrupole tandem mass spectrometer; Waters Ltd). Androstenedione was measured by tandem mass spectrometry using an in-house method. Thyroid function tests were assayed using the Abbott Architect platform (Abbott Laboratories). HbA1c was determined using a high-performance liquid chromatography (HPLC) assay (Tosoh HLC-723G8, Tosoh Corporation). The intra- and inter-assay coefficients of variation were all <9%.

A standard 75-g oral glucose tolerance test was performed in all participants to determine post-prandial insulin sensitivity. Glucose and insulin were measured at 0, 30, 60, 90, and 120 minutes. The areas under the curve (AUCs) for insulin and glucose were calculated using the trapezoid method. The homeostatic model assessment (HOMA) method was also used to estimate fasting insulin resistance (HOMA-IR) according to the formula (fasting insulin (mU/L) x fasting glucose (mg/dL)/405) [23].

155 **Isometric forearm contraction (IFC) protocol**

156 Isometric forearm contraction (IFC) at 30% maximum voluntary contraction was used to
157 generate a peripheral haemodynamic and SNS response. Maximum grip strength was
158 determined by asking the volunteer to squeeze an electronic hand dynamometer (90kg capacity
159 range) (Zhongshan Camry Electronic Co. Ltd, Guangdong, China) with their dominant hand to
160 maximum effort on three separate attempts, with a 60 second period of rest between each
161 squeeze, as previously recommended [24]. The mean maximum grip strength was determined
162 and 30% IFC subsequently calculated. This was then applied in a protocol which followed a
163 block design of 12 minutes in total, comprising 1 minute rest, 3 minutes squeeze, 2.5 minutes
164 rest, 3 minutes squeeze and 2.5 minutes rest. The subjects were cued for the rest and squeeze
165 periods, and targeted to sustain 30% IFC during the squeeze periods (figure 1).
166
167 **Sympathetic activity measurements**

168 *Blood pressure and heart rate*. Resting blood pressure (mmHg) and heart rate (beats/min) were
169 measured at baseline using an Omron HEM-907 blood pressure monitoring device (Omron
170 Healthcare UK Ltd) on the non-dominant arm and every 30 seconds throughout the 12 minute
171 IFC protocol. Mean arterial blood pressure (MAP) was calculated. The mean of the values at
172 rest were calculated as a pre-IFC blood pressure and heart rate, and the mean of values at the
173 end of each 3 minute squeeze to give a post-IFC blood pressure and heart rate.
174
175 *Plasma catecholamines*. Blood was drawn from the non-dominant arm of the subject in a
176 supine position after a 10 minute rest period (pre-IFC catecholamines). Following 3 minutes
177 of IFC at 30% maximum handgrip strength, further blood was drawn for post-IFC

178 catecholamines. Samples were centrifuged at 2000rpm at 4°C within 10 minutes of collection
179 and aliquots stored at -80°C until analysis. Catecholamines were measured using an
180 Epinephrine ELISA Kit (Abnova, Taoyuan County, Taiwan) and Norepinephrine ELISA Kit
181 (Abnova, Taoyuan County, Taiwan). The intra- and inter-assay coefficients of variation were
182 <15.4% and <16.1% respectively.

183

184 *Microneurography.* A subset of patients (n=7, age 29.6 ± 6.4 yrs, BMI 27.3 ± 4.9 kg/m²) and
185 controls (n=7, age 30.1 ± 6.2 yrs, BMI 27.1 ± 6.2 kg/m²) agreed to undergo microneurography.
186 Studies were conducted on a separate day between 0830 and 1530 hours in a quiet physiological
187 lab maintained at 20°C and performed by a single observer blind to subject status (YS). Direct
188 recordings of multiunit efferent postganglionic muscle sympathetic nerve activity (MSNA)
189 were obtained with a tungsten microelectrode with a tip diameter of a few micrometers inserted
190 into a muscle fascicle of the peroneal nerve, posterior to the fibular head. A low-impedance
191 reference electrode was inserted subcutaneously a few centimeters from the fibular head. When
192 a muscle nerve fascicle was identified, small electrode adjustments were made until a site was
193 found in which spontaneous, pulse-synchronous bursts of neural activity could be recorded.
194 Details of the nerve recording technique and criteria for MSNA have been reported previously
195 [25]. Bursts identified by inspection of the mean voltage neurogram were expressed as burst
196 frequency (number of pulse synchronic sympathetic bursts per minute) [bursts/min (BF)] and
197 burst incidence (number of pulse synchronic sympathetic bursts per 100 heart beats)
198 [bursts/100 heartbeats (BI)]. Total MSNA activity was measured to take into account both the

frequency and size of a sympathetic burst (the product of burst per minute and mean burst amplitude), expressed in arbitrary units. The total MSNA during the last 60 seconds of a rest period was used as a baseline to establish the percentage change in MSNA during the last 60 seconds of the 30% IFC.

MRI data acquisition

MRI was performed on a 3T GE HDx MRI system (General Electric). The head was held immobile in an eight-channel receive only head coil by foam pads. A continuous series of 232 fMRI image volumes (echo-planar images using BOLD contrast, scan time = 12 mins, TR = 3.1s, TE = 25ms) were collected for each run. In-plane voxel size was 1.5x1.5 mm^2, matrix 128x128x40 and Field-of-view (FOV) 192x192mm^2 in plane. The slice thickness was 2.2mm and slice gap 0.8mm. Each volume covered the entire brain and brainstem. Slices were tilted 10°-15° from the axial to the coronal plane to reduce signal loss due to dephasing in the brainstem resulting from through-slice susceptibility-induced gradients [26]. Structural images were collected using a T1-weighted sequence in order to facilitate visualization.

Blood oxygen level-dependent (BOLD) fMRI scan protocol

The scan protocol aimed to reveal BOLD signal correlates with the IFC task, using a block design. Subjects were fitted with a nasal cannula to measure end tidal CO_2. Respiration pattern was determined by a strain-gauge band around the chest. Heart rate was measured from a pulse oximeter on the left hand (MedRad, USA). Physiological data were collected with a computer-

based data acquisition and analysis system (CED 1401, Cambridge, UK). An in-house MRI-compatible handgrip device was positioned in the dominant hand and connected to a pressure transducer. The pressure signal was collected with a computer-based data acquisition and analysis system (CED 1401, Cambridge, UK) and displayed on a screen located inside the scanner. Subjects followed visual instructions presented on the screen as to the rest and squeeze periods, with a target bar showing when 30% squeeze had been achieved. PsychoPy version 1.78 [27] was used to run the visual stimulus. Subjects performed the previously described block paradigm twice with time to rest between the runs.

Image and statistical analyses

Analysis of the scans was by FEAT (fMRI Expert Analysis Tool, version 6.00) software (available on-line at www.fmrib.ox.ac.uk/fsl). Each T1 scan was registered to the MNI152, an average T1 brain image constructed from 152 normal subjects at the Montreal Neurological Institute (MNI), Montreal, QC, Canada, using linear registration (FLIRT within the FMRIB Software Library (FSL)) [28-29]. The functional BOLD scans were then registered to each individual's T1 structural image. fMRI images were un-warped, motion corrected and spatially smoothed. Physiological noise from cardiac and respiratory signals was retrospectively regressed out from the images. FSL contains the software FLIRT (FMRIB's Linear Image Registration Tool) that allowed the linear transformation of imaging data [28, 30]. A high-pass filter of 330 seconds was used. To generate contrast images, task-related BOLD activation was estimated with a design matrix specifying a general linear model (GLM) that included a waveform based on each person's IFC recording obtained during the scan protocol from the hand grip device. The visual stimulus shown in the scan session was also included in this analysis. BOLD signal changes for blood pressure condition were modelled with a waveform derived from the blood pressure recordings made out of scanner during the 12-minute

paradigm. Z statistic images were thresholded using clusters determined by $z > 2.3$ and a cluster significance threshold of $P = 0.05$ [31]. Significant BOLD signal intensity changes were color coded and rendered onto an individual's T1-weighted anatomic image set. The resulting statistical parametric maps were used in higher level analysis to determine differences between PCOS and control groups. As the paradigm was run twice, an intermediate level FEAT analysis was run for each subject by combining their two lower-level FEAT outputs, to produce an average for each subject. These were then used in the higher-level FEAT analysis that could be used in the group analyses to examine BOLD activation in the PCOS and control groups and the differences in activation between groups ($z > 2.3$, $p=0.05$).

For the pressor, MSNA and catecholamine responses, statistical analysis was performed using SPSS version 20.0 (IBM, New York). An independent-samples t-test was used to compare the difference between the PCOS and control group means. A p-value of <0.05 was considered statistically significant.

Results

Baseline characteristics

Table 1 shows the clinical, anthropometric and metabolic characteristics of the two groups. The groups were closely matched for age, BMI, resting heart rate and blood pressure. Testosterone and androstenedione levels were non-significantly higher in PCOS subjects than controls. Similarly, the insulin response to oral glucose challenge (insulin AUC) and HOMA-IR values were higher in PCOS subjects but fell just short of statistical significance. Triglyceride levels in the PCOS group were higher than in controls.

Sympathetic activity measurements

Pressor response

19 PCOS and 19 controls had heart rate (HR) and blood pressure (BP) measured in response to the IFC paradigm (table 2). As anticipated, IFC induced a significant rise in HR and BP in both groups. However, there were no between-group differences in the HR or BP increase from baseline in response to IFC.

Catecholamines

The plasma catecholamine response to IFC was assessed in 39 subjects (20 PCOS, 19 controls) (table 2). Mean resting catecholamine concentrations were not different between groups. Following IFC, norepinephrine levels did not change but epinephrine concentrations increased significantly in the PCOS group ($p<0.001$). However, differences between groups in epinephrine response to IFC were not apparent.

MSNA

Resting data were obtained from 16 subjects (8 PCOS, 8 controls). Only 14 of these (7 PCOS, 7 controls) were able to proceed with full MSNA recordings post-IFC due to technical difficulties, including inability to locate the peroneal nerve for recordings (n=1) and a participant who was unable to keep their leg in position (n=1).

Resting burst frequency (BF), burst incidence (BI) and total MSNA was not different between groups (table 2). The increase in BF was significantly greater (68%) in the PCOS group compared to controls (11.9%; p=0.002). The increases in BI (PCOS: 55.4%, controls: 20.5%) and total MSNA (PCOS: 124.1%, controls: 86.4%) were not significantly different between groups.

fMRI BOLD signal activation

30 participants (15 PCOS, 15 controls) underwent fMRI scanning with out-of-scanner HR and BP changes recorded every 30 seconds in response to the IFC paradigm. There were no significant differences in the age, BMI, testosterone, HOMA-IR, resting HR or resting BP between groups. The change in BOLD signal intensity that fitted the modelled blood pressure response showed activation in the PCOS group in the right cerebral cortex, right pallidum, right thalamus and right parietal operculum cortex ($p<0.0001$) and control group in the intracalcarine cortex and lingual gyrus (p=0.003). BOLD signal activation was significantly greater in the PCOS group compared to controls in the right orbitofrontal cortex ($p<0.0001$), and less so in the left angular gyrus and lateral occipital cortex (p=0.04) (figures 2(a) and 2(b)). No differences were observed in the brainstem.

Metabolic influences on fMRI BOLD signal change

When the BOLD signal change modelled for hemodynamic response was adjusted for variance associated with testosterone, using testosterone as a covariate at the group level, BOLD activation in the right orbitofrontal cortex was still greater in the PCOS group compared to controls ($p<0.0001$). However, when the BOLD signal was separately adjusted for insulin sensitivity (HOMA-IR), the BOLD signal differences between groups in the right orbitofrontal cortex were no longer significant. When corrected for HOMA-IR, the BOLD signal in the left angular gyrus and lateral occipital cortex remained significant.

Discussion

Our study demonstrates that women with PCOS have evidence of enhanced sympathoexcitation in response to IFC compared to age- and BMI-matched controls, and that this is accompanied by a difference in BOLD signal change that localizes to the right orbitofrontal cortex. This finding is consistent with previous studies implicating this region in the neural control of blood pressure [17, 32, 33], but to our knowledge is the first to confirm enhanced activation in this region in young women with insulin resistance. These observations may extend our understanding of the mechanisms involved in neurogenic hypertension in young 'at risk' subjects.

In common with many previous studies, we used IFC at 30% of maximum grip as our stimulus to induce a blood pressure rise. In young adult volunteers this has been shown not to increase nociception [18]. The pressor response we observed was of a similar magnitude to other studies [18, 34-35] and did not differ between women with PCOS and controls. This is in keeping with observations in patients with type 2 diabetes whereby systolic and diastolic blood pressure rose in parallel to controls in response to IFC, despite differences in resting blood pressure between groups [36].

We did not observe any rise in concentrations of the sympathetic neurotransmitter norepinephrine in either group but plasma measurement offers limited sensitivity and reproducibility, unlike radiolabelled techniques which may be used reliably to measure regional sympathetic activity in individual organs. Furthermore, plasma norepinephrine measurement cannot distinguish between increased central catecholamine production and

366 reduced clearance [37]. For these reasons, the significance of the greater rise in plasma
367 epinephrine concentrations in the PCOS group following IFC is uncertain.
368
369 In contrast to plasma catecholamines, microneurography represents a more direct measurement
370 of sympathetic neural output. In common with many studies, we chose the common peroneal
371 nerve, in view of its easy accessibility, to measure efferent MSNA. Importantly, MSNA
372 correlates well with autonomic effector (including blood pressure and heart rate) responses
373 [25], and provides immediate data on sympathetic output. However, it is invasive, hence we
374 were only able to recruit a proportion of our total group to this sub-study. Nevertheless, women
375 with PCOS showed a greater rise in burst frequency in response to IFC than controls, although
376 resting measures were not different between groups. This contrasts with previous studies,
377 where higher resting MSNA values were observed in women with PCOS [11-12]. However,
378 it is noticeable that the resting burst frequency and burst incidence values in our control group
379 were significantly greater than those reported in these previous studies, and this may go some
380 way to explain the absence of differences in MSNA between our two groups at baseline.
381
382 This study identified several cortical areas whose BOLD signal change correlated with the
383 modelled BP response to static exercise. Of these, between-group differences were most
384 apparent in the right orbitofrontal cortex. This cerebral region has previously been shown to
385 associate with a pressor response in humans. In a positron emission tomography study,
386 Critchley and colleagues identified the right orbitofrontal cortex as one of several brain regions
387 implicated in the cardiovascular response to isometric exercise and mental stress [17]. Harper
388 *et al.* used functional MRI to demonstrate increased activity in the right orbitofrontal cortex
389 during hypertension induced by cold pressor and Valsalva stimuli [33], whilst Gianaros *et al.*
390 showed that the orbitofrontal cortex was similarly activated in response to a behavioral stressor

391 [32]. More recently, Macefield and Henderson contemporaneously captured skin sympathetic
392 nerve activity (SSNA) directly during BOLD fMRI of the brain [38], showing correlation of
393 spontaneous SSNA with BOLD signal intensity in the right orbitofrontal cortex. Furthermore,
394 in animal studies, the orbitofrontal cortex has been shown to connect to the insular cortex, a
395 key regulator in the pressor response [39]. Our data therefore support the prevailing view that
396 a cortical and sub-cortical network exists in humans to control cardiovascular responses.
397 Studies in patients with intractable epilepsy undergoing intracranial electrode implantation and
398 deep brain stimulation appear to confirm this, whereby stimulation of the subcallosal
399 neocortex, which lies adjacent to the orbitofrontal cortex, elicited marked systolic hypotensive
400 changes likely as a result of reduced sympathetic drive [40].
401
402 In an attempt to understand the potential metabolic drivers of the altered BOLD signal
403 response, we extended our analyses to sequentially adjust for hyperandrogenism and insulin
404 resistance, observing that adjustment for HOMA-IR, but not testosterone, abolished the
405 between-group differences in BOLD signal intensity in the right orbitofrontal cortex. This
406 implies that differences in insulin sensitivity, and compensatory hyperinsulinemia, might
407 account for the differences we observed in the BOLD signal response in this area in response
408 to IFC. Our findings may thus have relevance for other metabolic disorders characterized by
409 insulin resistance, such as metabolic syndrome and type 2 diabetes, which we speculate might
410 similarly be affected by altered BOLD signal in this cerebral region. Although little insulin is
411 produced in the brain, insulin receptors are widely distributed in the brain and peripherally-
412 made insulin can cross the blood-brain barrier [41]. Furthermore, intracerebroventricular
413 injection of insulin in rodents induces sympathoexcitation via the arcuate nucleus [13, 42]. In
414 humans, hyperinsulinemia increases MSNA and modifies baroreflex control of sympathetic
415 activity [43-44] although these effects of insulin on sympathetic outflow may be blunted in

insulin-resistant states such as obesity and the metabolic syndrome [45-46]. We therefore speculate that the enhanced activation observed in the right orbitofrontal cortex in women with PCOS may reflect preserved insulin sensitivity in this cerebral region. This raises the possibility that insulin sensitization might have therapeutic benefit in reducing sympathetic output in PCOS and consequently improving cardiometabolic outcomes. Indeed, metformin caused a dose-dependent reduction in heart rate, blood pressure and renal sympathetic nerve activity in spontaneously hypertensive rats [49], but similar benefits were not observed short-term in obese hypertensive men [50]. In contrast, both rosiglitazone and pioglitazone have been shown to reduce sympathetic nerve activity in subjects with type 2 diabetes [51-52].

In contrast to other studies [18], we did not find any change in BOLD signal in the brainstem following IFC, a region that we hypothesized at the outset might be activated in response to this paradigm. In particular, medullary structures are implicated in autonomic control of cardiovascular responses. Reasons for this might include physiological noise due to cardiac and respiratory motion, and the presence of magnetic field inhomogeneity caused by the nearby sphenoid sinus. Furthermore, the small size of brainstem nuclei in humans [53] makes localization challenging even when using MRI scanners (3T) that image with greater resolution than conventional systems. In this regard, the enhanced signal and spatial resolution offered by 7T systems may offer an important advance.

Our study has some limitations. Firstly, we chose to define our subjects with PCOS by the Rotterdam criteria since this embraces a ‘milder’ metabolic phenotype characterized by lesser degrees of hyperandrogenism and insulin resistance than other definitions such as the NIH criteria [54]. Whilst this allowed us to explore the effects of relatively mild insulin resistance on cerebral and pressor responses to IFC, the study group was heterogeneous and it is difficult

to be certain if our findings extend to all sub-phenotypes of the syndrome; further studies are needed in this regard. Since patients with hyperandrogenic PCOS carry a worse cardiometabolic risk profile, we speculate that inclusion of patients with more severe hyperandrogenism may have exaggerated the differences we observed in orbitofrontal cortex activation and/or unmasked other cerebral regions implicated in the neurogenic regulation of blood pressure. Inclusion of a young population nevertheless avoids the potentially confounding influences of vascular pathology (from e.g. diabetes and hypertension) on blood flow and therefore BOLD signal. Secondly, MSNA and pressor recordings were undertaken out-of-scanner; it would have been preferable to do so during scanning, as demonstrated recently by others [20, 38] but this is beyond our current technical ability. Thirdly, our study used static hand grip to induce a pressor response, which is a motor task cued by a visual stimulus. Although the potential confounding influence of this model was reduced by factoring the motor and visual tasks into the FEAT analysis, we nevertheless observed a change in BOLD signal intensity in the intracalcarine cortex and lingual gyrus in controls, in the parietal operculum in subjects with PCOS, and between-group differences in the lateral occipital cortex and left angular gyrus, which are likely to relate to remaining confounding effects of the visual stimulus. Similarly, the signal change in the right thalamus, pallidum and cerebral cortex in the PCOS group may reflect residual confounding by the motor component of the hand grip task. However, imaging studies have also suggested that areas of the thalamus may be implicated in blood pressure control, potentially via increasing vagal tone and reducing sympathoexcitation [55].

In conclusion, our study supports previous observations of enhanced sympathetic output in women with PCOS but demonstrates for the first time that this is accompanied by regional differences in cerebral activation that are most marked in the right orbitofrontal cortex. This

466 differential activation appears to relate to altered insulin sensitivity, and suggests that
467 treatments targeted at reducing hyperinsulinemia in young women with PCOS may have
468 benefits in reducing sympathetic output and improving cardiovascular health.
469

470 **References**

471 1. Morgan CL, Jenkins-Jones S, Currie CJ, Rees DA. Evaluation of adverse outcome in young
472 women with polycystic ovary syndrome versus matched, reference controls: a retrospective,
473 observational study. *Journal of Clinical Endocrinology and Metabolism*. 2012; 97: 3251–3260.
474

475 2. Talbott E, Guzick D, Clerici A, Berga S, Weimer K, Kuller L. Coronary heart disease risk
476 factors in women with polycystic ovary syndrome. *Arterioscler Thromb Vasc Biol*. 1995; 15:
477 821-826.
478

479 3. Sampson M, Kong C, Patel A, Unwin R, Jacobs HS. Ambulatory blood pressure profiles and
480 plasminogen activator inhibitor (PAI-1) activity in lean women with and without the polycystic
481 ovary syndrome. *Clin Endocrinol (Oxf)*. 1996; 45: 623-629.
482

483 4. Paradisi G, Steinberg HO, Hempfling A, Cronin J, Hook G, Shepard MK, Baron AD.
484 Polycystic ovary syndrome is associated with endothelial dysfunction. *Circulation*. 2001; 103:
485 1410-1415.
486

487 5. Lansdown A, Rees DA. The sympathetic nervous system in polycystic ovary syndrome: a
488 novel therapeutic target? *Clinical Endocrinology.* 2012; 77: 791-801.

489

490 6. Yildirir A, Aybar F, Kabakci G, Yarali H, Oto A.. Heart Rate Variability in Young Women
491 with Polycystic Ovary Syndrome. *Ann Noninvasive Electrocardiol*. 2006; 11: 306-312.
492
493 7. Di Domenico K, Wiltgen D, Nickel FJ, Magalhães JA, Moraes RS, Spritzer PM. Cardiac
494 autonomic modulation in polycystic ovary syndrome: does the phenotype matter? *Fertil Steril*.
495 2013; 99(1): 286-92.
496
497 8. Saranya K, Pal GK, Habeebullah S, Pal P. Assessment of cardiovascular autonomic function
498 in patients with polycystic ovary syndrome. *J Obstet Gynaecol Res.* 2014; 40(1): 192-9.
499
500 9. Tekin G, Tekin A, Kiliçarslan EB, Haydardedeoğlu B, Katircibaşi T, Koçum T, Erol T,
501 Cölkesen Y, Sezgin AT, Müderrisoğlu H. Altered autonomic neural control of the
502 cardiovascular system in polycystic ovary syndrome. *Int J Cardiol*. 2008; 130: 49-55.
503
504 10. Giallauria F, Palomba S, Manguso F, Vitelli A, Maresca L, Tafuri D, Lombardi G, Colao
505 A, Vigorito C, Orio F. Abnormal heart rate recovery after maximal cardiopulmonary exercise
506 stress testing in young overweight women with polycystic ovary syndrome. *Clinical*
507 *Endocrinology*. 2008; 68: 88-93.
508
509 11. Sverrisdóttir YB, Mogren T, Kataoka J, Janson PO, Stener-Victorin E. Is polycystic ovary
510 syndrome associated with high sympathetic nerve activity and size at birth? *Am J Physiol*
511 *Endocrinol Metab*. 2008; 294: E576-E581.
512
513 12. Lambert EA, Teede H, Sari CI, Jona E, Shorakae S, Woodington K Hemmes R, Eikelis N,
514 Straznicky NE, De Courten B, Dixon JB, Schlaich MP, Lambert GW. Sympathetic activation

and endothelial dysfunction in polycystic ovary syndrome are not explained by either obesity or insulin resistance. *Clin Endocrinol (Oxf).* 2015; 83(6): 812-9.

13. Cassaglia PA1, Hermes SM, Aicher SA, Brooks VL. Insulin acts in the arcuate nucleus to increase lumbar sympathetic nerve activity and baroreflex function in rats. *J Physiol*. 2011; 589(Pt 7):1643-62.

14. Mark AL1, Agassandian K, Morgan DA, Liu X, Cassell MD, Rahmouni K. Leptin signaling in the nucleus tractus solitarii increases sympathetic nerve activity to the kidney. *Hypertension.* 2009; 53(2): 375-80.

15. Resstel LB1, Corrêa FM. Involvement of the medial prefrontal cortex in central cardiovascular modulation in the rat. *Auton Neurosci*. 2006; 126-127:130-8.

16. Krämer HH, Ament SJ, Breimhorst M, Klega A, Schmieg K, Endres C, Buchholz HG, Elam M, Schreckenberger M, Birklein F. Central correlation of muscle sympathetic nerve activation during baroreflex unloading - a microneurography-positron emission tomography study. *Eur J Neurosci.* 2014; 39(4): 623-9.

17. Critchley HD, Corfield DR, Chandler MP, Mathias CJ, Dolan RJ. Cerebral correlates of autonomic cardiovascular arousal: a functional neuroimaging investigation in humans. *Journal of Physiology.* 2000; 523(1): 259-270.

538 18. Coulson JM, Murphy K, Harris AD, Fjodorova M, Cockcroft JR, Wise RG. Correlation
539 between baseline blood pressure and the brainstem fMRI response to isometric forearm
540 contraction in human volunteers: a pilot study. *J Hum Hypertens*. 2015; 29(7): 449-55.
541
542 19. Macefield VG, Henderson LA. Real-time imaging of the medullary circuitry involved in
543 the generation of spontaneous muscle sympathetic nerve activity in awake subjects. Hum Brain
544 Mapp 2010; 31(4):539-549.
545
546 20. Macefield VG, James C, Henderson LA. Identification of sites of sympathetic outflow at
547 rest and during emotional arousal: concurrent recordings of sympathetic nerve activity and
548 fMRI of the brain. *Int J Psychophysio*l. 2013; 89(3): 451-9.
549
550 21. Rotterdam ESHRE/ASRM-Sponsored PCOS Consensus Workshop Group Revised 2003
551 consensus on diagnostic criteria and long-term health risks related to polycystic ovary
552 syndrome (PCOS). *Hum Reprod,* 2004; 19: 41–47
553
554 22. Watson S, Blundell HL, Evans WD, Griffiths H, Newcombe RG, Rees DA. Can abdominal
555 bioelectrical impedance refine the determination of visceral fat from waist circumference?
556 *Physiol Meas*. 2009; 30: N53–N58.
557
558 23. Matthews DR, Hosker JP, Rudenski AS, Naylor BA, Treacher DF, Turner RC. Homeostasis
559 model assessment: insulin resistance and beta-cell function from fasting plasma glucose and
560 insulin concentrations in man. *Diabetalogia*. 1985; 28: 412–419.
561

562 24. Innes E. Handgrip strength testing: A review of the literature. *Australian Occupational*
563 *Therapy Journal.* 1999; 46: 120-140.
564
565 25. Vallbo AB, Hagbarth KE, Torebjörk HE, Wallin BG*l.* Somatosensory, proprioceptive and
566 sympathetic activity in human peripheral nerves. *Physiol Rev*. 1979; 59: 919– 957.
567
568 26. Weiskopf N, Hutton C, Josephs O, Deichmann R. Optimal EPI parameters for reduction of
569 susceptibility-induced BOLD sensitivity losses: a whole-brain analysis at 3T and 1.5T.
570 *Neuroimage*. 2006; 33(2): 493-504.
571
572 27. Peirce JW PsychoPy - Psychophysics software in Python. J *Neurosci Methods*. 2007;
573 162(1-2): 8-13
574
575 28. Jenkinson M and Smith SM. A global optimisation method for robust affine registration of
576 brain images. *Medical Image Analysis*. 2001; 5(2):143-156.
577
578 29. Jenkinson M. Fast, automated, N-dimensional phase-unwrapping algorithm. *Magn Reson*
579 *Med.* 2003; 49(1): 193-7.
580
581 30. Jenkinson M, Bannister PR, Brady JM, Smith SM. Improved optimisation for the robust
582 and accurate linear registration and motion correction of brain images. *NeuroImage*. 2002;
583 17(2): 825-841.
584

585 31. Worsley KJ. Statistical analysis of activation images (Chapter 14). In: Jezzard P, Matthews
586 PM, Smith SM (ed). *Functional MRI: An Introduction to Methods*. New York: Oxford
587 University Press. 2001.
588
589 32. Gianaros PJ, May JC, Siegle GJ, Jennings JR. Is there a functional neural correlate of
590 individual differences in cardiovascular reactivity? *Psychosom Med.* 2005; 67(1): 31-9.
591
592 33. Harper RM, Gozal D, Bandler R, Spriggs D, Lee J, Alger J. Regional brain activation in
593 humans during respiratory and blood pressure challenges. *Clinical Experimental*
594 *Pharmacology and Physiology.* 1998; 25: 483–486.
595
596 34. Stewart JM, Montgomery LD, Glover JL, Medow MS. Changes in regional blood volume
597 and blood flow during static handgrip. *Am J Physiol Heart Circ Physiol*. 2007; 292: H215-
598 H223.
599
600 35. Goodwin GM, McCloskey DI, Mitchell JH. Cardiovascular and respiratory responses to
601 changes in central command during isometric exercise at constant muscle tension. *J Physiol.*
602 1972; 226(1): 173-190.
603
604 36. Petrofsky JS1, Stewart B, Patterson C, Cole M, Al Malty A, Lee S. Cardiovascular
605 responses and endurance during isometric exercise in patients with Type 2 diabetes compared
606 to control subjects. *Med Sci Monit*. 2005; 11(10): CR470-7.
607
608 37. Grassi G and Esler M. How to assess sympathetic activity in humans. *J Hypertension*. 1999;
609 17: 719-734.

610

611 38. Macefield VG, Henderson LA. “Real-time” imaging of cortical and subcortical sites of
612 cardiovascular control: concurrent recordings of sympathetic nerve activity and fMRI in awake
613 subjects. *J Neurophysiol.* 2016; 116(3): 1199-207.

614

615 39. Cavada C, Company T, Tejedor J, Cruz-Rizzolo RJ, Reinoso-Suárez F. The anatomical
616 connections of the macaque monkey orbitofrontal cortex. *Cerebral Cortex*. 2000; 10: 220–42.

617

618 40. Lacuey N, Hampson JP, Theeranaew W, Zonjy B, Vithala A, Hupp NJ, Loparo KA, Miller
619 JP, Lhatoo SD. Cortical Structures Associated With Human Blood Pressure Control. *JAMA*
620 *Neurol*. 2018; 75(2): 194-202.

621

622 41. Hopkins DF, Williams G. Insulin receptors are widely distributed in human brain and bind
623 human and porcine insulin with equal affinity. *Diabet Med.* 1997 Dec; 14(12): 1044-50.

624

625 42. Rahmouni K1, Morgan DA, Morgan GM, Liu X, Sigmund CD, Mark AL, Haynes WG.
626 Hypothalamic PI3K and MAPK differentially mediate regional sympathetic activation to
627 insulin. *J Clin Invest.* 2004; 114(5): 652-8.

628

629 43. Vollenweider P1, Tappy L, Randin D, Schneiter P, Jéquier E, Nicod P, Scherrer U.
630 Differential effects of hyperinsulinemia and carbohydrate metabolism on sympathetic nerve
631 activity and muscle blood flow in humans. *J Clin Invest*. 1993; 92(1): 147-54.

632

633 44. Young CN, Deo SH, Chaudhary K, Thyfault JP, Fadel PJ. Insulin enhances the gain of
634 arterial baroreflex control of muscle sympathetic nerve activity in humans. *J Physiol*. 2010;
635 588(Pt 18): 3593-603.
636
637 45. Vollenweider P1, Randin D, Tappy L, Jéquier E, Nicod P, Scherrer U. Impaired insulin-
638 induced sympathetic neural activation and vasodilation in skeletal muscle in obese humans.
639 *J Clin Inv*est. 199; 93(6): 2365-71.
640
641 46. Straznicky NE, Lambert GW, Masuo K Dawood T, Eikelis N, Nestel PJ, McGrane MT,
642 Mariani JA, Socratous F, Chopra R, Esler MD, Schlaich MP, Lambert EA. Blunted sympathetic
643 neural response to oral glucose in obese subjects with the insulin-resistant metabolic syndrome.
644 *Am J Clin Nutr*. 2009; 89: 27-36.
645
646 49. Petersen JS, DiBona GF. Acute sympathoinhibitory actions of metformin in spontaneously
647 hypertensive rats. *Hypertension*. 1996; 27(3 Pt 2): 619-25.
648
649 50. Gudbjörnsdottir S, Friberg P, Elam M, Attvall S, Lönnroth P, Wallin BG. The effect of
650 metformin and insulin on sympathetic nerve activity, norepinephrine spillover and blood
651 pressure in obese, insulin resistant, normoglycemic, hypertensive men. *Blood Press*. 1994;
652 3(6): 394-403.
653
654 51. Yosefy C, Magen E, Kiselevich A, Priluk R, London D, Volchek L, Viskoper RJ Jr.
655 Rosiglitazone improves, while Glibenclamide worsens blood pressure control in treated
656 hypertensive diabetic and dyslipidemic subjects via modulation of insulin resistance and
657 sympathetic activity. *J Cardiovasc Pharmacol*. 2004; 44(2): 215-22.

658

659 52. Kobayashi D1, Takamura M, Murai H, Usui S, Ikeda T, Inomata J, Takashima S, Kato T,
660 Furusho H, Takeshita Y, Ota T, Takamura T, Kaneko S. Effect of pioglitazone on muscle
661 sympathetic nerve activity in type 2 diabetes mellitus with α-glucosidase inhibitor. *Auton*
662 *Neurosci.* 2010; 158(1-2): 86-91.

663

664 53. Guyenet PG. The sympathetic control of blood pressure. *Nat Rev Neurosci*. 2006; 7(5):
665 335-46.

666

667 54. Daan NM, Louwers YV, Koster MP, Eijkemans MJ, de Rijke YB, Lentjes EW, Fauser BC,
668 Laven JS. Cardiovascular and metabolic profiles amongst different polycystic ovary syndrome
669 phenotypes: who is really at risk? *Fertil Steril*. 2014; 102(5): 1444-1451.

670

671 55. Kimmerly DS, O'Leary DD, Menon RS, Gati JS, Shoemaker JK. Cortical regions
672 associated with autonomic cardiovascular regulation during lower body negative pressure in
673 humans. *J Physiol*. 2005; 569(Pt 1): 331-45.

674 **Tables and figures.**

675 **Table 1.** Anthropometric and metabolic characteristics of the study population

	PCOS (n=20)* Mean ± SD	**Control (n=20) Mean ± SD**	**p- value**
Age (yrs)	29.80 ± 4.78	29.65 ± 4.96	0.92
BMI (Kg/m²)	26.05 ± 4.90	26.11 ± 4.83	0.97
WHR	0.88 ± 0.07	0.84 ± 0.04	0.04
Waist circumference (cm)	85.9 ± 13.7	85.1 ± 11.1	0.86
Hip circumference (cm)	97.2 ± 10.4	101.4 ± 11.8	0.24
Testosterone (nmol/L)	1.41 ± 0.77	1.03 ± 0.53	0.09
Androstenedione (nmol/L)	4.51 ± 2.99	3.64 ± 1.28	0.25
HbA1c (mmol/mol)	34.15 ± 2.76	34.21 ± 2.64	0.95
Total cholesterol (mmol/L)	5.22 ± 1.05	4.79 ± 0.55	0.12
Triglycerides (mmol/L)	1.34 ± 0.68	0.90 ± 0.36	0.02
Insulin AUC (pmol min/L)	55519.50 ± 41547.67	35320.26 ± 21008.31	0.07
Glucose AUC (mmol min/L)	764.85 ± 239.02	661.89 ± 219.03	0.17
HOMA-IR	1.41 ± 1.10	0.88 ± 0.65	0.08
Resting HR (beats/min)	71.05 ± 8.59	71.26 ± 7.65	0.94
Resting SBP (mmHg)	114.53 ± 9.33	117.58 ± 12.62	0.40
Resting DBP (mmHg)	65.16 ± 13.33	65.47 ± 14.31	0.94
Resting MAP (mmHg)	81.63 ± 11.26	83.84 ± 10.54	0.54

676 BMI, body mass index; AUC, area under the curve during oral glucose tolerance test;

677 HOMA-IR, homeostatic model assessment of insulin resistance. *19 controls underwent an

678 oral glucose tolerance test

679

680

681 **Table 2.** Pressor, catecholamine and MSNA responses to IFC in PCOS and control groups

	PCOS Mean ± SD			Controls Mean ± SD			p-value PCOS vs controls
	Pre-IFC	**Post-IFC**	**p-value**	**Pre-IFC**	**Post-IFC**	**p-value**	
Pressor response	**n=19**			**n=19**			
HR (beats/min)	71.05 ± 8.59	76.68 ± 8.04	<0.001	71.26 ± 7.65	75.11 ±8.43	<0.001	0.155
SBP (mmHg)	114.53 ± 9.33	127.11 ± 13.69	<0.001	117.58 ± 12.62	125.84 ± 11.21	<0.001	0.090
DBP (mmHg)	65.16 ± 13.33	74.84 ± 15.79	<0.001	65.47 ± 14.31	74.21 ± 10.68	<0.001	0.157
MAP (mmHg)	81.63 ± 11.26	92.37 ± 13.97	<0.001	83.84 ± 10.54	91.32 ± 9.27	<0.001	0.058
Catecholamines	**n=20**			**n=19**			
Epinephrine concentration (ng/mL)	0.68 ± 0.53	1.23 ± 0.71	<0.001	0.77 ± 0.59	0.99 ± 0.61	0.14	0.32
Norepinephrine concentration (ng/mL)	18.11 ± 11.18	16.77 ± 10.01	0.38	22.99 ± 13.33	20.99 ± 12.12	0.25	0.42
MSNA	**n=7**			**n=7**			
BF (bursts/min)	25.9 ± 4.4	42.9 ± 8.2	0.001	29.6 ± 7.1	34.9 ± 4.5	0.149	0.002
BI (bursts/100 heartbeats)	36.3 ± 9.9	54.4 ± 12.1	0.004	42.0 ± 10.3	47.9 ± 7.1	0.199	0.133
Total MSNA	2.4 ± 1.3	5.5 ± 3.1	0.004	2.6 ± 0.7	4.4 ± 1.7	0.048	0.420

682 HR, heart rate; SBP, systolic blood pressure; DBP, diastolic blood pressure; MAP, mean arterial pressure; MSNA, muscle sympathetic nerve
683 activity; BF, burst frequency; BI, burst incidence.
684
685 **Legends for figures**
686 **Figure 1.** 12 minute IFC paradigm comprising 1 minute rest, 3 minutes 30% IFC, 2.5 minutes rest, 3 minutes 30% IFC and 2.5 minutes rest. The
687 timings of MSNA, catecholamine, heart rate and blood pressure measurements are indicated.
688
689 **Figure 2.** BOLD signal activation (modelled for blood pressure) differences between PCOS and controls in the right orbitofrontal cortex (a) and
690 between PCOS and controls in the left angular gyrus and lateral occipital cortex (b). The significant region is displayed with a threshold of
691 $Z>2.3$, with a cluster probability threshold of $p<0.05$.
692

693

694

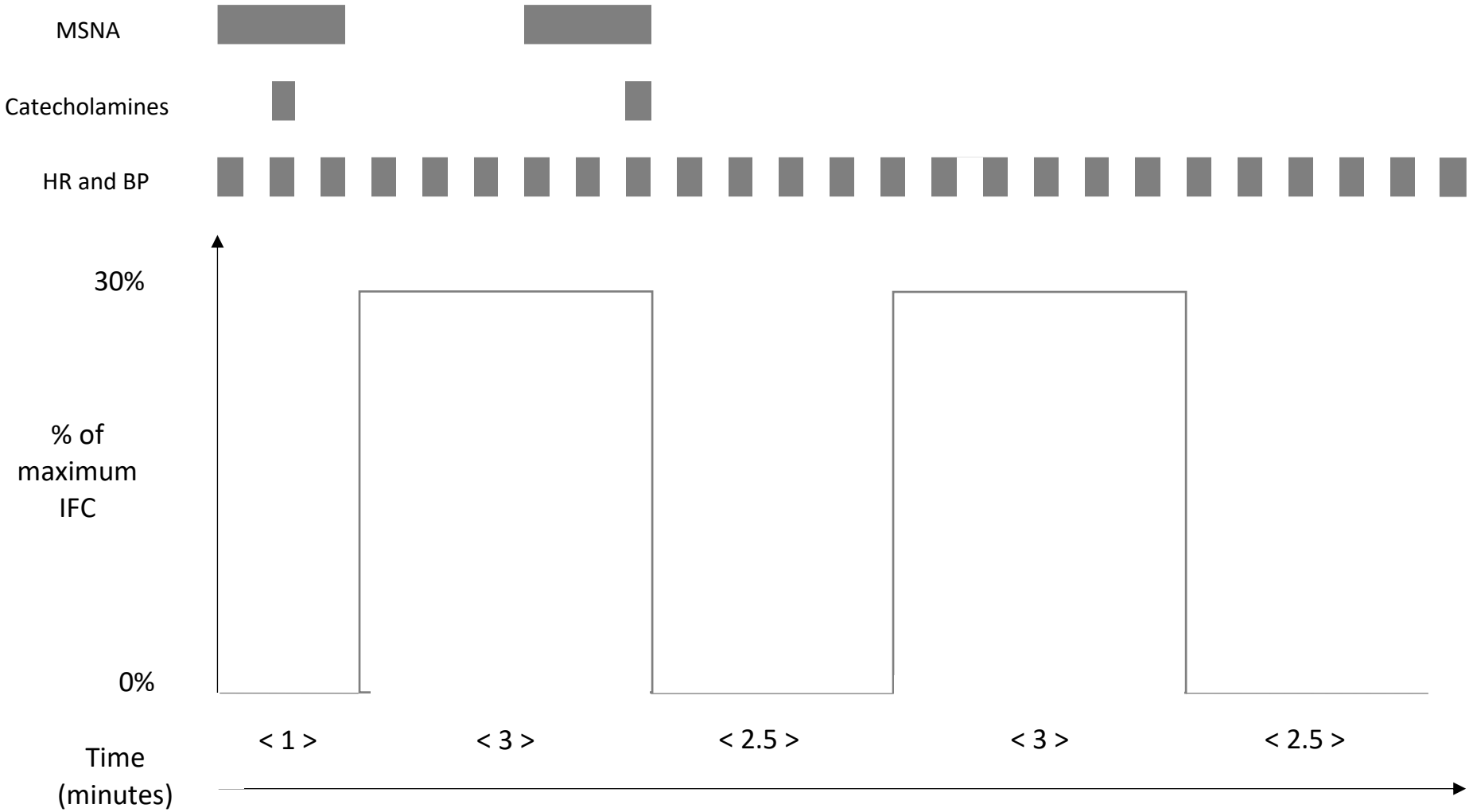
MSNA
Catecholamines
HR and BP
30%
% of maximum IFC
0%
< 1 >
< 3 >
< 2.5 >
< 3 >
< 2.5 >
Time (minutes)

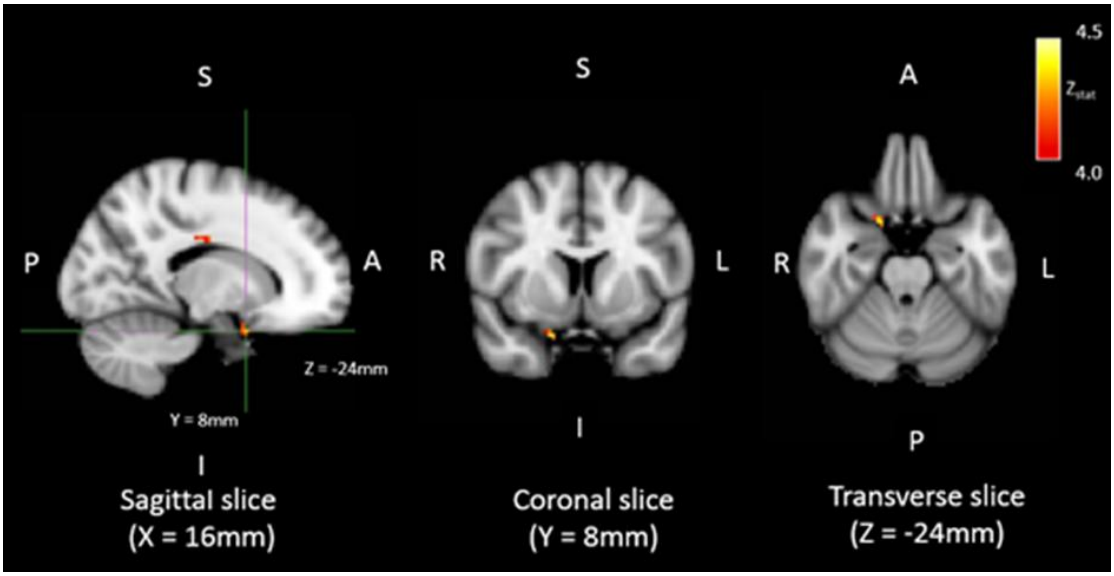
S
P
A
Z = -24mm
Y = 8mm
I
Sagittal slice
(X = 16mm)
S
R
L
I
Coronal slice
(Y = 8mm)
A
R
L
P
Transverse slice
(Z = -24mm)
4.5
Zstat
4.0

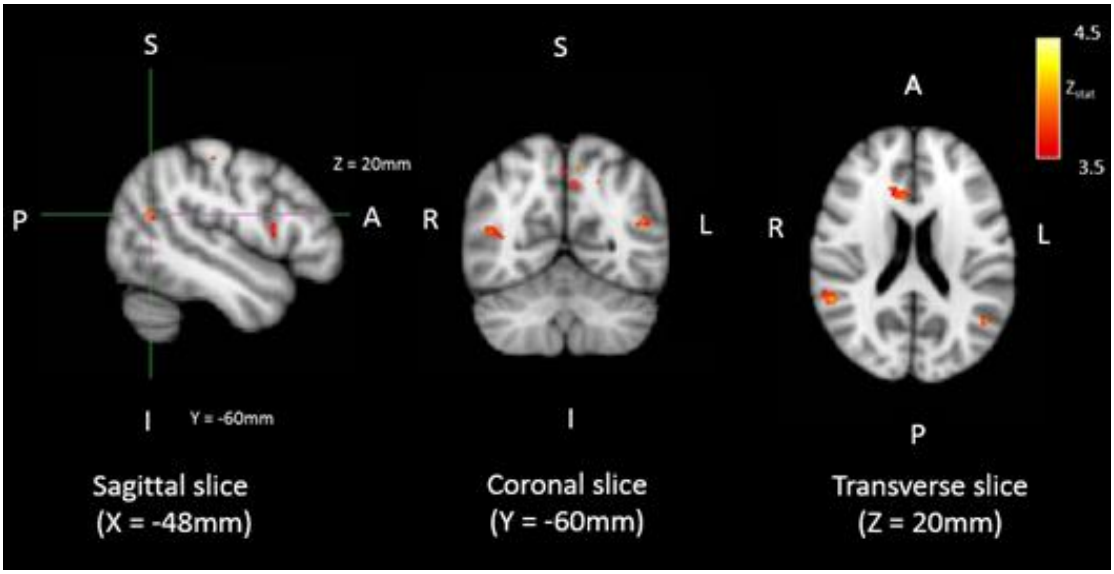
S
P
A
Z = 20mm
I
Y = -60mm
Sagittal slice
(X = -48mm)
S
R
L
I
Coronal slice
(Y = -60mm)
A
R
L
P
Transverse slice
(Z = 20mm)
4.5
Zstat
3.5